Optimization of defected ZnO/Si/Cu$_2$O heterostructure solar cell

Samah Boudour [a,b], Idris Bouchama [b,*], Moufdi Hadjab [a], Samiha Laidoudi [a]

[a] *Thin Films Development and Applications Unit UDCMA, Setif – Research Center in Industrial Technologies CRTI, B. O. Box 64, Cheraga, 16014, Algiers, Algeria*
[b] *Electronic Department, Faculty of Technology, University of Msila, Msila, 28000, Algeria*

ARTICLE INFO

ABSTRACT

In the present work, we review the optimization of the performance of a newly defected ZnO/Si/Cu$_2$O hetero-junction solar cell using the Analysis of Microelectronic and Photonic Structures (AMPS-1D) computer simulator under the AM1.5G illumination and the operating temperature of 300 K. The light J-V characteristics were investigated by varying the input parameters and the temperature. The use of p-type Cu$_2$O-back layer in the structure is to enhance the open-circuit voltage (V_{OC}). The performance of ZnO/Si/Cu$_2$O heterojunction solar cell is studied in order to optimize the layers parameters, such as the thickness of p-Si absorber layer, the doping and the defects concentrations of the p-Si absorber layer and to obtain an efficient proposed structure. The defects concentration of p-Si absorber layer was fixed in the first step at N_{def}(p-Si) $= 10^{14}$/cm^3. With the optimized p-Si layer parameters, an efficiency of 16.23% was obtained with J_{SC} ~26.25 mA/cm^2, V_{OC} ~0.72 V and FF~0.85 for n-ZnO window (0.1 μm)/p-Si Absorber (10 μm)/p-Cu$_2$O (0.1 μm) heterostructure. For N_{def}(p-Si) lower than 10^{14}/cm^3, the AMPS-1D simulation showed an appreciable performance. For N_{def}(p-Si) $= 10^{11}$/cm^3 we estimate best characteristics of about: J_{SC} ~27.57 mA/cm^2, V_{OC} ~0.78 V, FF~0.90 and Eff ~ 21.78%.

1. Introduction

Intrinsic or doped, either by oxygen vacancies or by substitution of some of the atoms, zinc oxide (ZnO) and cuprous oxide (Cu$_2$O) based semiconductors have received increasing concern because of their strong points of earth-abundance, non-toxicity, tunable optical band gap, low-cost in resources and ease of processing by versatile technology routes. Such pulse laser deposition [1], sol gel [2], electrodeposition [3], spray [4,5], sputtering [6,7] and other methods [8,9] are potential technologies offers a range of versatile new features and enhancements that meet the needs of ZnO and Cu$_2$O based applications. So far a large number of studies have been widely conducted to apply ZnO and Cu$_2$O semiconductors in broad applications such as gas sensors [10,11], glucose sensors [12,13], photocatalyst [14–16], photodegradation sensors [17–20], photoelectrochemical sensors [21], photoluminescence sensors [17,22,23], conductive switching [24] and photovoltaic (PV) devices [25–29].

ZnO thin films are electrically a high n-type conductive and optically an excellent transparent (85%) in the visible range. Furthermore, they have wide energy band gap of around ~3.37 eV at room temperature with high carrier concentration, where they act extensively as most suitable n-type partner with common p-type thin films such as Cu$_2$O [25,

29], CIGS [30], CdTe [31] and silicon [32]. In addition, Cu$_2$O thin films are non-stoichiometric, electrically natural p-type conductive and optically absorbing in the short-wavelength considered amount (~10^4/cm) of the luminous spectrum as they have direct energy band gap of 1.9–2.1 eV [18,26,33] with low carrier concentrations of ~10^{-16} cm^{-3} at room temperature [9]. However, the low photovoltaic efficiency of metal oxide-based photovoltaics is still challenging. In other words, ZnO and Cu2O based semiconductors are still under further development in order to become suitable candidates for new photovoltaic heterostructures. Up till now, the achieved practical power conversion efficiencies of the most common ZnO/Cu$_2$O heterojunction solar cells are remained significantly at lower percentages of ~6% because of some drawbacks, such as the non-ideal band alignment between the two heterojunction-sides and the defects within the layers [34–37]. Nevertheless, the sufficient electrical and optical properties of Cu$_2$O thin films strongly nominate them to other PV-uses. In particular, to enhance the open-circuit voltage (V_{OC}) by adding Cu$_2$O back-layer in CuO based solar cells, the one dimensional simulation of Zhu et al. [38] has shown that the conversion efficiency increased from 19% for a non-defected TiO$_2$/CuO two-layer structure to 28.5% for a non-defected TiO$_2$/-CuO/Cu$_2$O three-layers structure. Considering the enormous use of the robust and expensive crystalline silicon materials in advanced photonics

---

* Corresponding author. Tel.: +213 671 38 16 48.
E-mail address: idris.bouchama@univ-msila.dz (I. Bouchama).
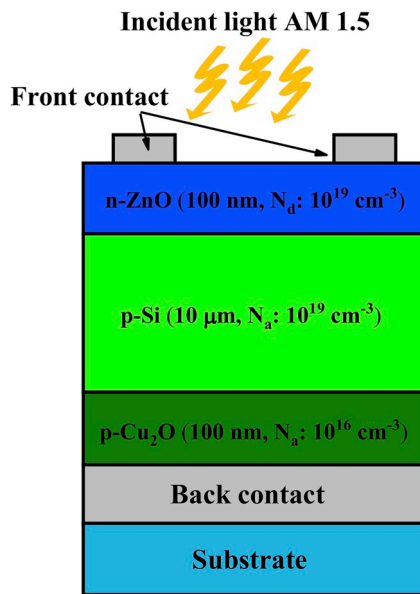
Fig. 1. Schematic of the newly ZnO/Si/Cu$_2$O heterostructure solar cell.

(SCAPS) and using an absorber of 1 μm of CIGS backed by 1 μm of crystalline silicon (c-Si) thin film in order to minimize the indium and gallium constituents, Heriche et al. [30] have reported conversion efficiency of 21.3%. In addition, because of its transparency and excellent electrical properties, ZnO has been integrated as n-type partner with p-type silicon to fabricate low cost thin film solar cells. Currently, the achieved practical power conversion efficiencies of the ZnO/Si hetero-junction solar cells are also remained at modest percentages, under 8.5% [39,40]. This modesty is likely due to the strong dependence of the common ZnO/Si heterojunction performance on the properties of deposited ZnO films. Here, ZnO/Si/Cu$_2$O heterojunction has high harvest of photons because of its double distinct p-type band gaps. The incident photons having energies smaller than the band gap of ZnO and greater than the band gap energy of Si will be absorbed near the depletion region as they competently transmit through the ZnO window. Those photons who have absorption length longer than the absorber

and electronics, it should be advisable to motivate the present-day extensively studied materials such as the TCOs and chalcopyrite thin films by using them as partners or supporters, side by side with thin films of crystalline silicon. Recently, based on one-dimensional simulator

Table 1
Settings for ZnO, Si and Cu$_2$O layers used in the simulation.

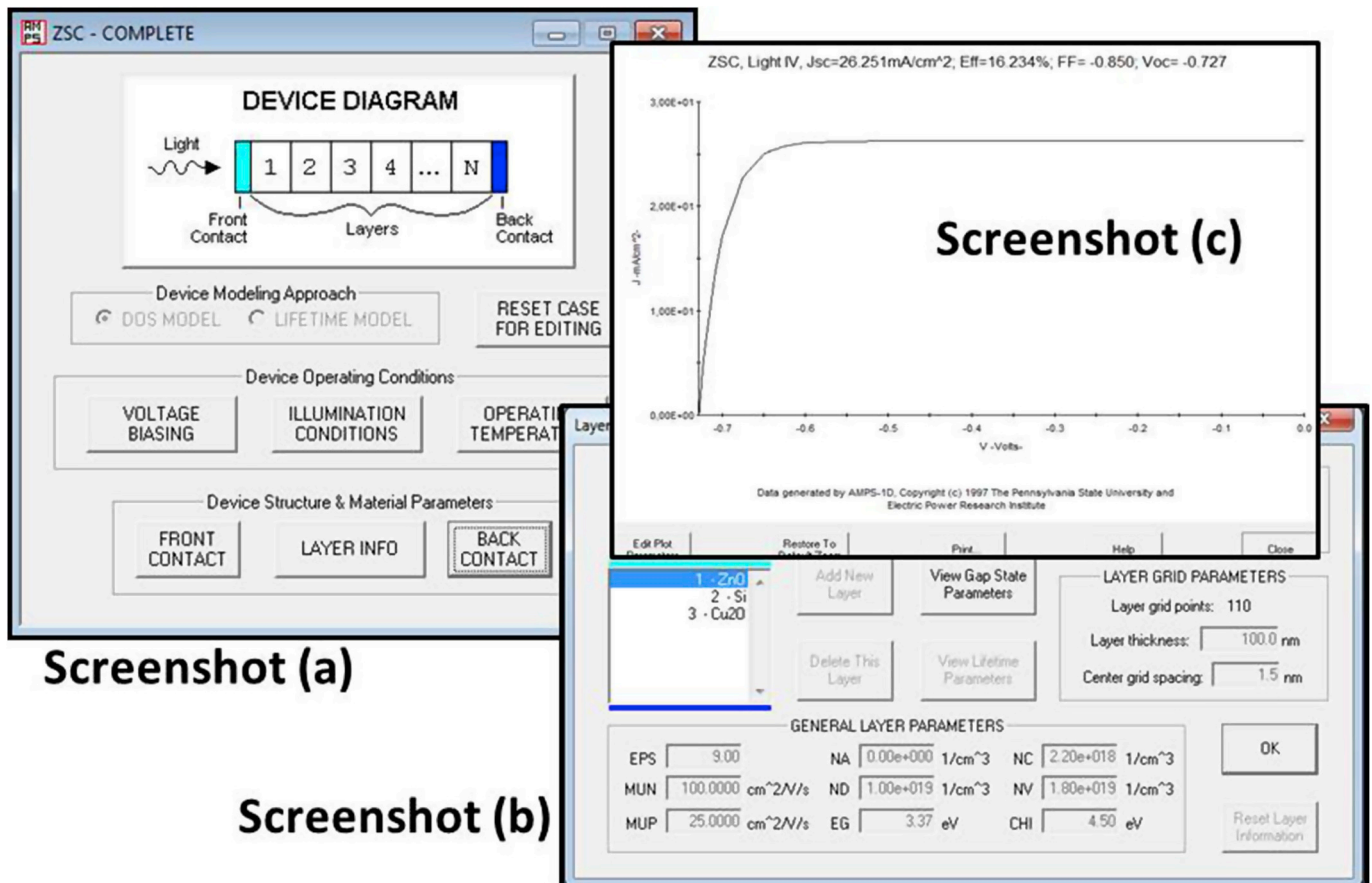| Parameters	n-ZnO	p-Si	p-Cu$_2$O
w (μm)	0.1	10	0.1
$\varepsilon/\varepsilon_0$	9.0	11.9	9.0
E_g(eV)	3.37	1.12	2.1
$N_{a,d}$(cm^{-3})	N_d: 1×10^{19}	N_a: 1×10^{19}	N_a: 1×10^{16}
χ_e(eV)	4.5	4.05	3.2
μ_n(cm^{2}V^{-1}s^{-1})	100.0	1450	20.0
μ_p(cm^{2}V^{-1}s^{-1})	25.0	500	40.0
N_c(cm^{-3})	2.22×10^{18}	2.80×10^{19}	2.20×10^{18}
N_v(cm^{-3})	1.8×10^{19}	2.65×10^{19}	1.11×10^{19}
N_{def}(cm^{-3})	1×10^{14}	1×10^{14}	1×10^{14}

Fig. 2. Typical data input panels of the AMPS-1D graphical user interface, allowing to set the solar cell device and its settings.
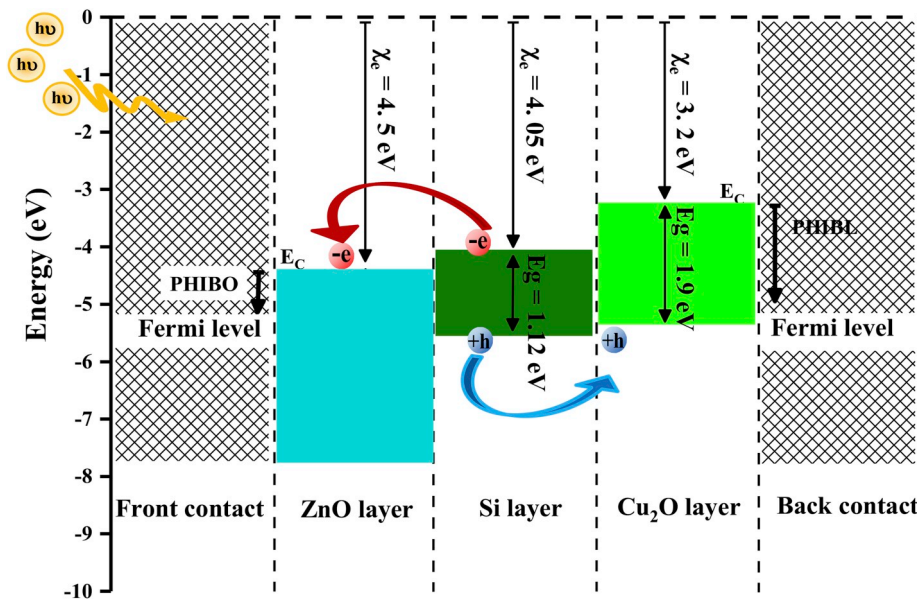
Fig. 3. Separated layers-energy level diagram of ZnO/Si/Cu$_2$O solar cell heterostructure.
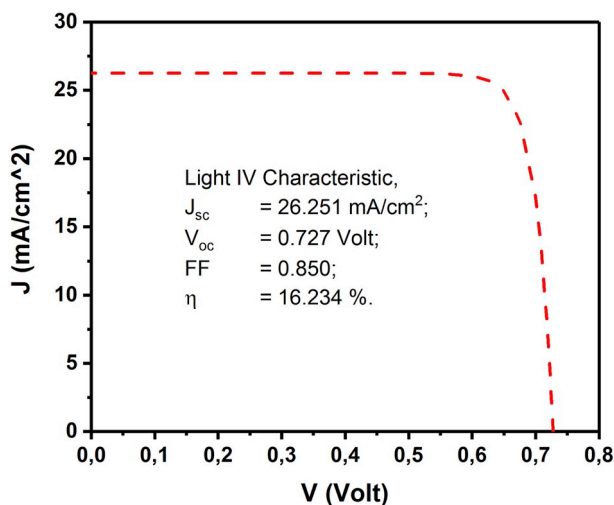

Fig. 4. Light J-V curve of the 0.1 μm-ZnO/10 μm-Si/0.1 μm-Cu$_2$O solar cell.

interlayer thickness and successfully traveled in the thin film Si inter-layer will be absorbed into Cu$_2$O back layer. The Cu$_2$O back layer itself will be also acting as barrier layer between p-Si material and the back contact to enhance the open circuit voltage V_{OC} [38] of the ZnO/Si heterojunction.

To avoid wasting resources, effort and time, solar cell community need to understand, explain and solve the physic and technology interferences of solar cell devices by using numerical simulators [30,31, 40,41]. These requirements have been reflected on the development of solar cells in which diverse abundant/non-abundant and low/high-cost materials, as well as their large influencing parameters, have been explored to renovate solar cell devices. The freely available Analysis of Microelectronic and Photonic Structures (AMPS-1D) one dimensional program was developed in 1990's by professor Fonash's team at the Pennsylvania State University [42].

In this paper, AMPS-1D simulator was considered to optimize a newly proposed defected ZnO/Si/Cu$_2$O heterojunction solar cell. The structure is analyzed numerically by changing different input parameters of the device such as thickness, doping and defect densities, and temperature. We examine the structural templates ZnO/Si/Cu$_2$O by light J-V characteristics and their electrical parameters: the short circuit current (J_{SC}), the open circuit voltage (V_{OC}), the fill factor (FF) and the efficiency (η).

2. Device settings and simulation process

Fig. 1 shows schematic of the newly proposed n-ZnO/p-Si/p-Cu$_2$O heterostructure solar cell. In order to analyze the transport physics in this structure, AMPS-1D solves the dipolar problems of device according to the Poisson equation and the continuity equations for electrons and holes. AMPS-1D simulator is a software environment, which is used to emulate a real solar cell behavior. In general, the simulation process would have to go through the following steps described by the screen-shots in Fig. 2. The screenshot (a) shows the typical information input panel of the AMPS-1D graphical user interface for simulation process of solar cell. The input buttons in this panel allow to specify the model of simulation and to access to the device operating conditions and the device structure and material parameters panels. The DOS mode is chosen for the device simulation. The screenshot (b) demonstrates the structure and the set of the material parameters of one particular layer as well as the input buttons of optical properties and defects. The screen-shot (c) shows the results of light J-V characteristics visualized in the form of curve and axes. During simulation handling, the AM1.5 illumi-nation spectrum with incident power of 100 mW/cm^2 is considered. The input parameters of each layer of the proposed structure have been summarized in Table 1. These parameters were the thickness, t, permittivity constant $\varepsilon/\varepsilon_0$, band gap E_g, electron affinity χ_e, electron/hole mobility μ_n/μ_p, effective density of states in conduction/valence band N_c/N_v, donor/acceptor concentration N_D/N_A, defect concentration N_{def} and the absorption coefficient in the range wavelength of 320–1100 nm. At the front contact, the reflection was neglected. The thermal velocity recombinations for holes/electrons S_n/S_p at front and back contacts were $1.0 \times 10^7 \, cm/s$. In Addition, the barrier height po-tentials $PHIBO$ and $PHIBL$ were considered Ohmic or slight Schottky barrier. As shown in Fig. 3, $PHIBO$ ($PHIBL$) is the difference between the work function of the metal front-contact (back-contact) and the electron affinity of the semiconductor in contact [E_C-E_F] with the unit of eV at front (back) contact.
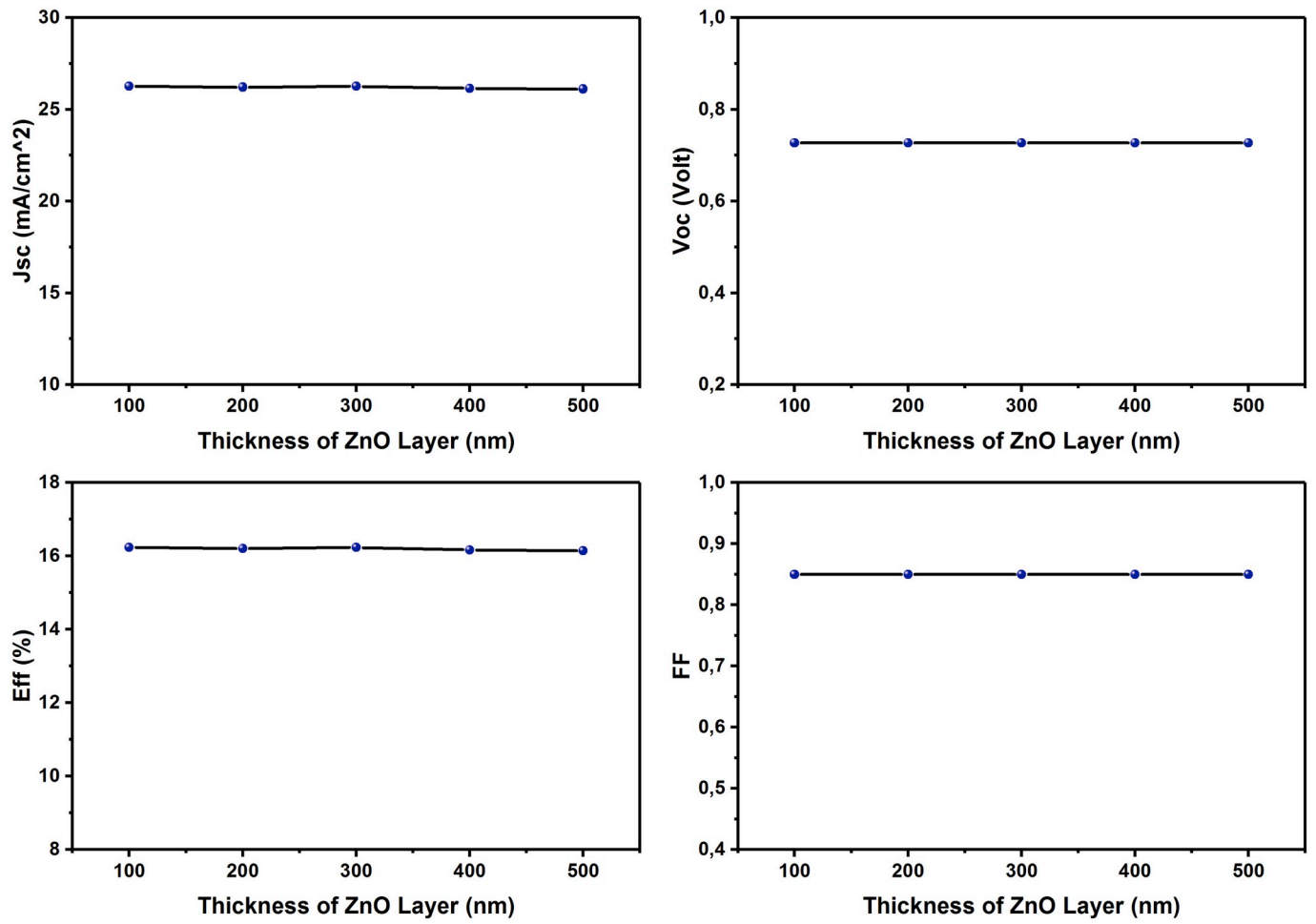
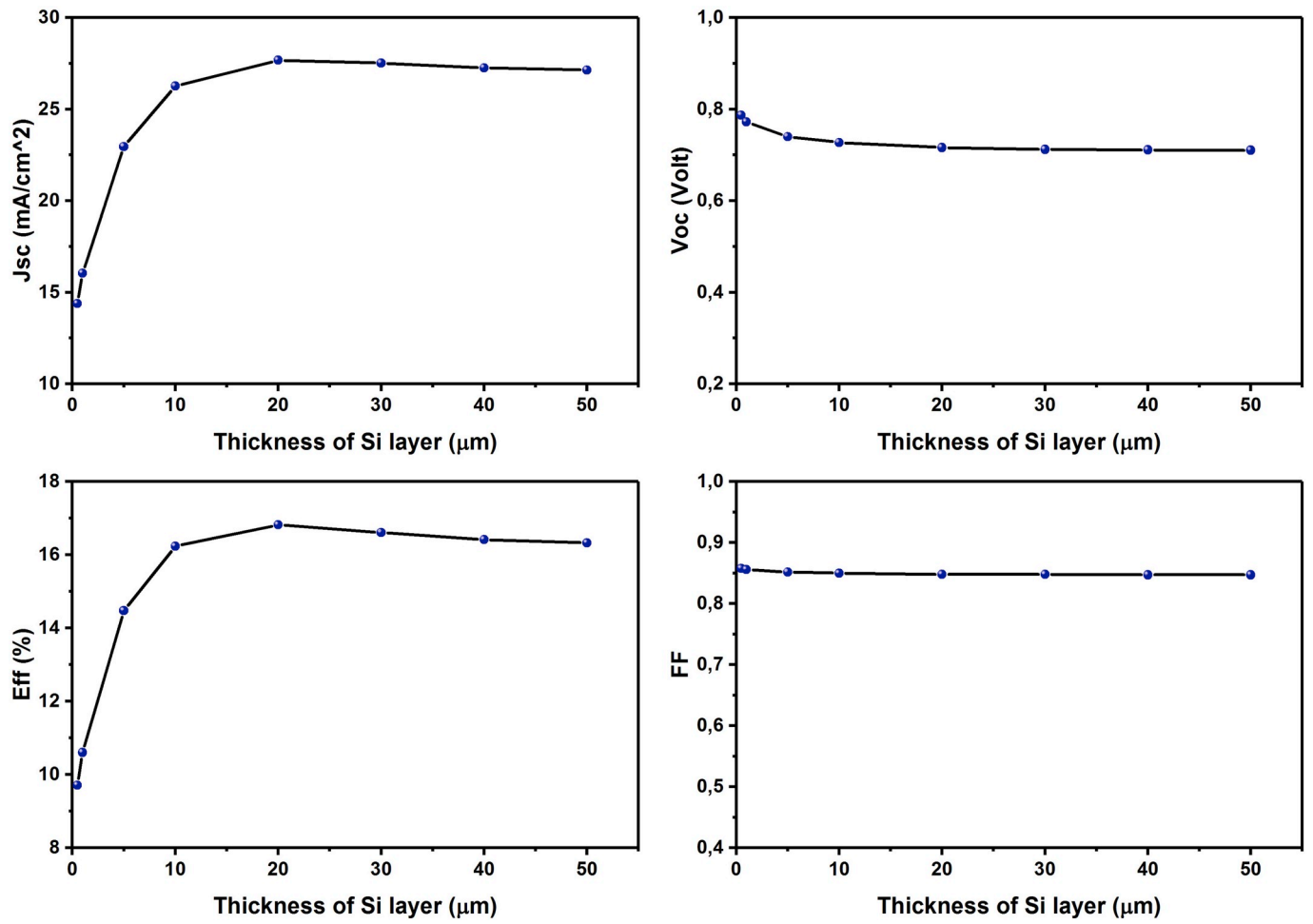**Fig. 5.** Photovoltaic parameters of defected $ZnO/Si/Cu_2O$ solar cell as a function of ZnO window layer thickness.

Fig. 6. Photovoltaic parameters of defected ZnO/Si/Cu$_2$O solar cell as a function of p-Si absorber layer thickness.
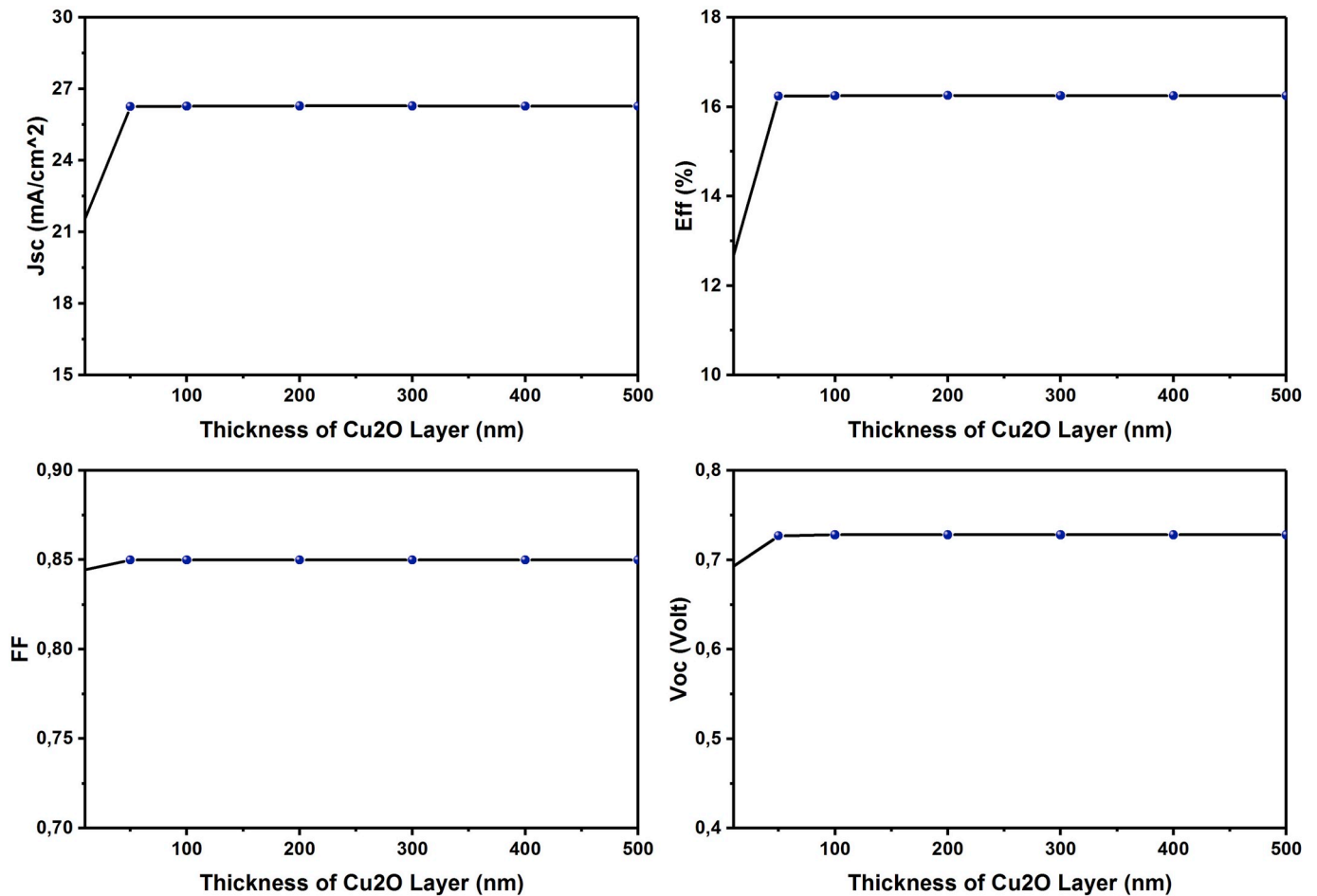
Fig. 7. Photovoltaic parameters of defected ZnO/Si/Cu$_2$O solar cell as a function of p-Cu$_2$O back layer thickness.

3. Results and discussion

In this section, we will examine the performance of the ZnO/Si/Cu$_2$O solar cell based on the settings summarized in Table 1. Fig. 3 shows the separated energy levels diagram for the ZnO, Si, Cu$_2$O layers. The conduction band offset (ΔE_C) at the ZnO/Si junction is the difference between the electron affinities of the ZnO and Si semiconductors: $\Delta \chi = \chi_{Si}$ - $\chi_{ZnO} = -0.45$ eV. The obtained cliff will allow the transport of photo-generated electrons to get form p-Si absorber layer to ZnO emitter layer before they recombine. On the other hand, the small valence band offset (ΔE_V) for Si/Cu$_2$O is found to be about -0.07 eV [($\chi_{Cu2O} + E_{gCu2O}$) - ($\chi_{Si} + E_{gSi}$) = -0.07eV]. Therefore, this established semi-alignment will allow the holes flowing through the rear contact. Thus, there is a good alignment between ZnO and Si and between Si and Cu$_2$O.

The light current density-voltage (J-V) characteristics are the fitting of current density versus the voltage. Based on the settings mentioned in Table 1, the light J-V curve and its characteristics, are shown in Fig. 4. The defect concentration of p-Si absorber layer was fixed at N_{def}(p-Si) = 10^{14}/cm^3. It has been demonstrated a good performance: η ~16.234% with J_{SC} ~26.251 mA/cm^2, V_{OC} ~0.727 V and FF ~0.85.

3.1. Effect of the ZnO layer thickness on the cell performance

Fig. 5 summarizes the effect of the ZnO window layer thickness on the performance of the ZnO/Si/Cu$_2$O solar cell from 100 nm to 500 nm. As shown in Fig. 5, all J-V characteristics remain unchanged and a fixed efficiency of about 16.2% was obtained, with J_{SC} ~26.2 mA/cm^2, V_{OC}

~0.72 V and FF ~0.85. This behavior is a result of the deficient carrier generation in the ZnO layer due to its wide band-gap energy of 3.37 eV.

3.2. Thickness optimization of p-Si absorber layer

Fig. 6 shows the evolution patterns of V_{OC}, J_{SC}, FF and η of ZnO/Si/Cu$_2$O solar cell as a function of p-Si absorber layer thickness from 0.5 µm to 50 µm. Particularly, J_{SC} and η increase rapidly from 14.37 to about 26.25 mA/cm^2 (by ~ 45.23%) and from 9,71 to about 16.23% (by ~ 40.17%), respectively, when the Si-layer thickness increases from 0.5 to 10 µm. While, V_{OC} (~0.7 V) and FF (~0.85) are almost unchanged. For a thick p-Si absorber layer (more than 10 µm), all photovoltaic parameters have almost unchanged values. This overall behavior is resulted from the increase of the photons absorption and even the increase of the electron-hole generation in the p-Si absorber layer. Therefore, the thickness of 10 µm is chosen as an optimum thickness for p-Si absorber layer for efficient ZnO/Si/Cu$_2$O solar cell. This is consistent with what has been found in previous research. It was reported that 10–50 µm thick c-Si based solar cells can have conversion efficiencies up to ~17%. Reuter et al. [43] reported that an efficiency of 17% is achieved on mono-crystalline silicon solar with thickness of approximately 47 µm, which is fabricated by using transfer layer process. Yoon et al. [44] reported an efficiency of about 17.5% within 15 µm thick crystalline Si solar cells. Cruz-Campa et al. [45] obtained an efficiency of 14.9% within 14 µm thick crystalline silicon solar cells. Li et al. [46] attempted to demonstrate that tandem ultra-thin a-Si/c-Si solar cells with a nanopyramid structure could obtain efficiencies as high as 13.3% within
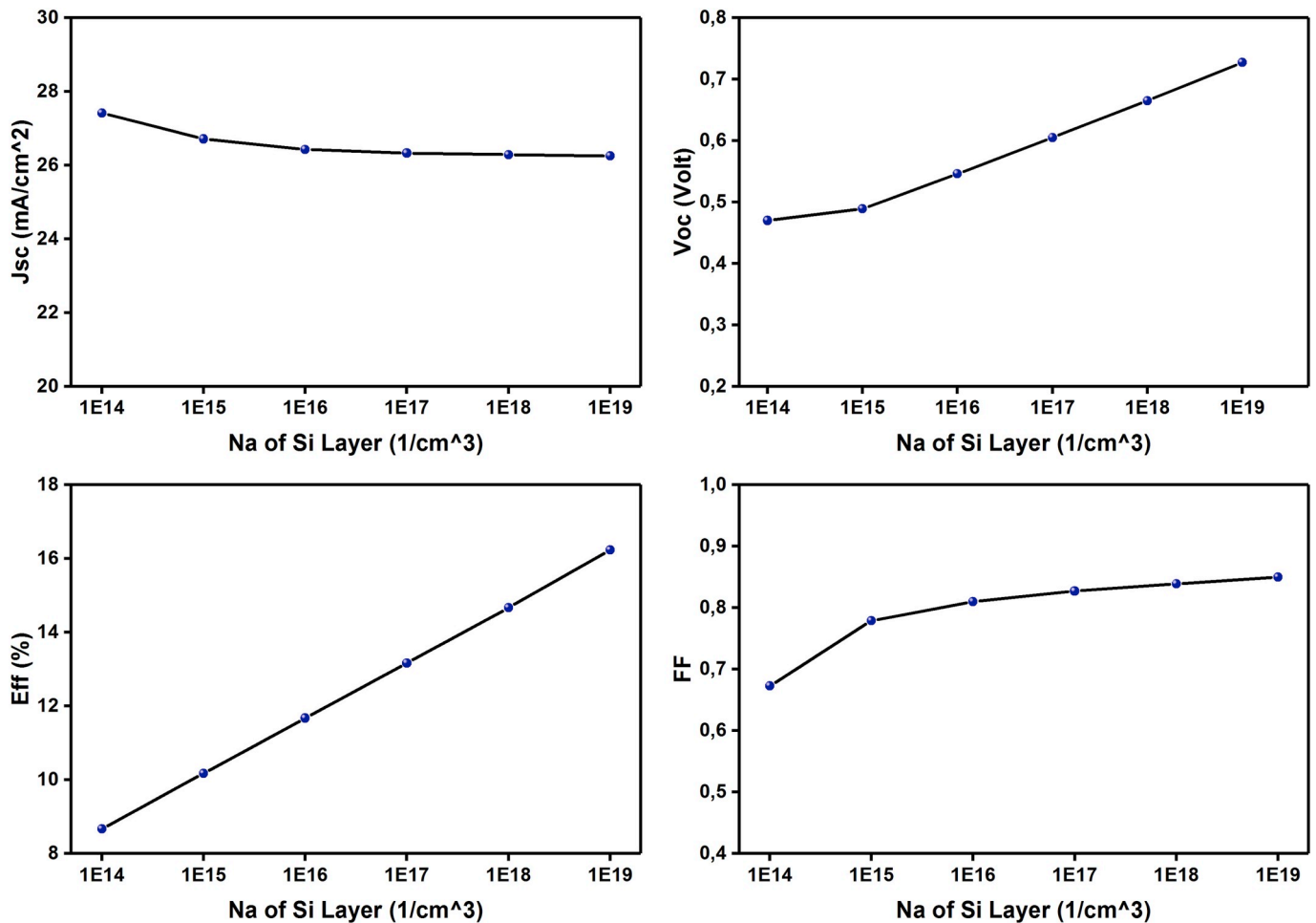
Fig. 8. Photovoltaic parameters of defected ZnO/Si/Cu$_2$O solar cell as a function of doping concentration N_A(p-Si).

only 8 μm thick silicon solar cells.

3.3. Thickness optimization of Cu$_2$O back layer

To clarify the effect of the Cu$_2$O back layer thickness (from 0 nm to 500 nm) on the cell performance, the ZnO/Si/Cu$_2$O heterostructure was simulated and the results are summarized in Fig. 7. At 0 nm thick (without Cu$_2$O layer), the photovoltaic parameters are initially low with J_{SC} ~20.42 mA/cm^2, V_{OC} ~0.68 V, FF ~0.84 and an efficiency of about 11.77%. In the presence of a Cu$_2$O layer with an increased thickness, all J-V characteristics remain unchanged at a good efficiency η of about 16.2%, with J_{SC} ~26.2 mA/cm^2, V_{OC} ~0.72 V and FF ~0.85. Therefore, a few μm of Si layer give more chances to a few nm of Cu$_2$O back layer (several hundred nm to few μm for most experimental Cu$_2$O based solar cells [47,48]) to absorb the photons who have absorption length longer than the p-Si interlayer thickness. Thus, a high efficiency of about 16.2% has been expected.

3.4. Optimization of acceptor density of p-Si absorber layer

Fig. 8 shows the evolution patterns of J_{SC}, V_{OC}, FF and η of ZnO/Si/Cu$_2$O solar cell versus different acceptor concentrations of p-Si absorber layer, N_A(p-Si). For lowest and/or highest doping concentrations (N_A(p-Si) $< 10^{14}$/cm^3 and/or N_A(p-Si) $> 10^{19}$/cm^3), N_A(p-Si) have a large impact on the electronic properties (mobility, conductivity/resistivity and related parameters) of crystalline silicon. Consequently, N_A(p-Si)

was varied in a moderate range from 1×10^{14}/cm^3 to 1×10^{19}/cm^3 [49]. When N_A(p-Si) exceed the effective density of states N_v(p-Si) (~10^{19}/cm^3), the crystalline silicon becomes degenerate semi-conductor, thus the energy band-gag narrowing will be [50].

At the beginning, for N_A(p-Si) = 1×10^{14}/cm^3 the efficiency η and FF were achieved small values of about 8.67% and 0.67, respectively. For N_A(p-Si) $> 1 \times 10^{14}$/cm^3, we observe that J_{SC} shows slight decrease from 27.41 mA/cm^2 at the concentration 1×10^{14}/cm^3 to 26.25 mA/cm^2 at the concentration 1×10^{19}/cm^3. In contrast, the open circuit voltage, V_{OC}, shows a considered increase from 0.47 V at the concentration 1×10^{14}/cm^3 to 0.72 V at the concentration 1×10^{19}/cm^3. For N_A(p-Si) = 1×10^{19}/cm^3, the efficiency η and FF were increased to about 16.23% and 0.85, respectively. The recommended acceptor density N_A(p-Si) should be higher than that of its defect density (in this case 1×10^{14}/cm^3).

3.5. Effect of Gaussian defects of ZnO/Si/Cu$_2$O heterostructure

Simulation results for ZnO/Si/Cu$_2$O heterostructure with different gaussian (both of acceptor-like and donor-like) defects located in the band gap of p-Si absorber layer are shown in Fig. 9. From this figure, the defect density, N_{def}(p-Si), shows harmful effects on the ovarall performance of the device. The highest possible values of J-V charactistics were obtained when N_{def}(p-Si) $< 1 \times 10^{14}$/cm^3. At lower defects concentration N_{def}(p-Si) = 1×10^{11}/cm^3 the corresponding characteristics were: J_{SC} ~ 27.57 mA/cm^2, V_{OC} ~ 0.78 V, FF ~ 0.90 and η ~ 21.78%.
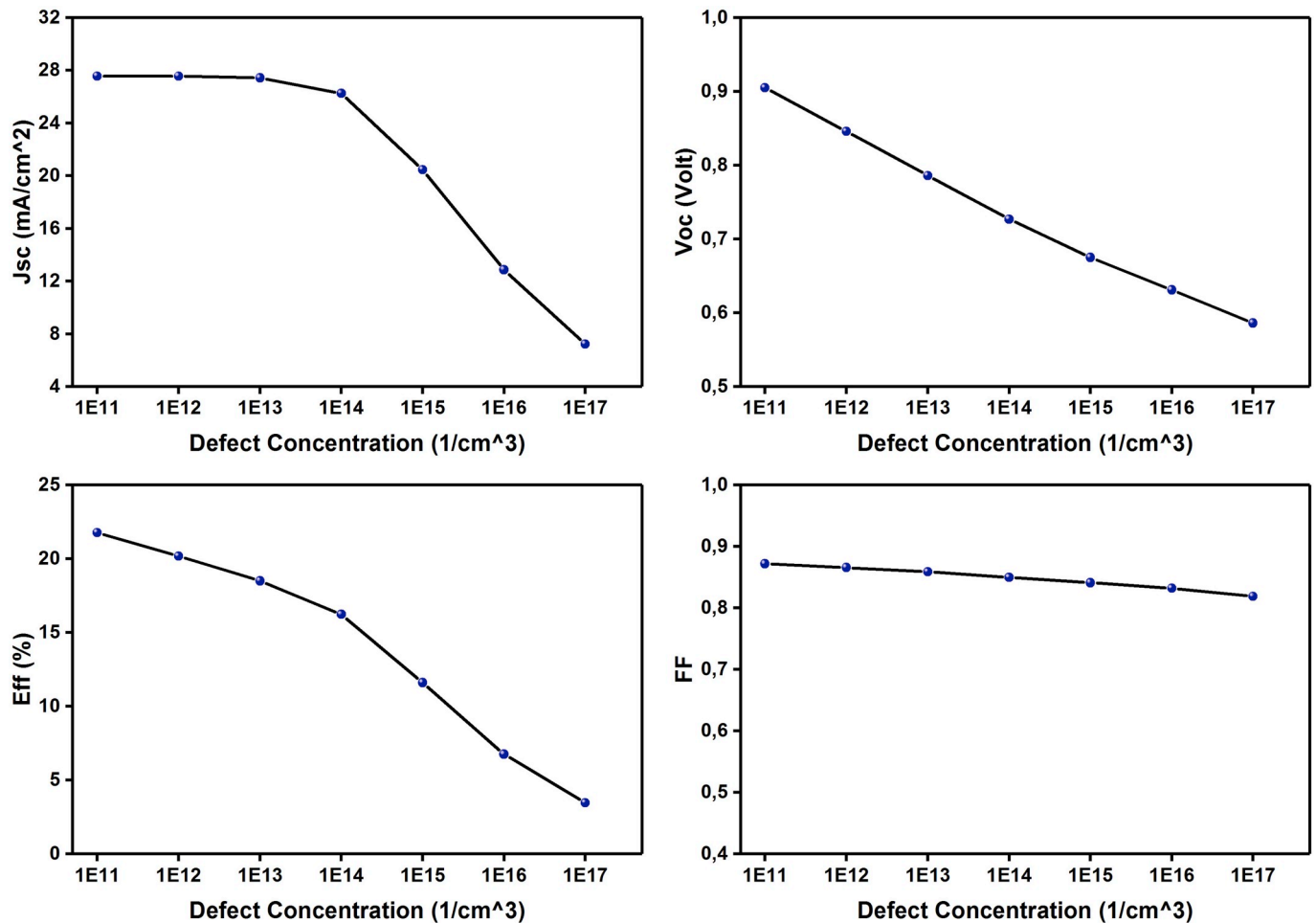
Fig. 9. Photovoltaic parameters of defected $ZnO/Si/Cu_2O$ solar cell as a function of defects concentration N_{def}(p-Si).

Increasing N_{def}(p-Si) more than 1×10^{14}/cm^3, the J_{SC} and V_{OC} were significantly affected. The defect concentration of 1×10^{17}/cm^3 caused a sharp fall in the J-V charactristics: J_{SC} ~7.23 mA/cm^2, V_{OC} ~0.58 V, FF ~0.82 and η ~3.46%. This poor behavior of the $ZnO/Si/Cu_2O$ device at high bulk defects is resulted from recombination phenomena. Therefore, the current transport may severely affected by the bulk defect density of the layer. This effect is related to created trapping (recombination) in the bulk layer that limits the efficiency [51].

3.6. Operating temperature effect on ZnO/Si/Cu₂O heterostructure performance

In the literature, the dependence of the V_{OC} to the operating temperature is used as an indicator on the stability of solar cells [30]. To testify this vital dependence on the defected $ZnO/Si/Cu_2O$ hetero-structure solar cell, the operating temperature is stepped from 300 K to 600 K by 50 K. Fig. 10 shows the evolution pattern of the photovoltaic parameters as a function of the operating temperature. Generally, increasing the operating temperature conduct to a decrease of material band gap and eventually an increase to the leakage current and a decrease to the V_{OC}. The current density J_{SC} has almost unchanged pattern (~26.5 mA/cm^2). From Fig. 10, V_{OC} decreased from ~0.73 V (recorded at 300 K) to ~ 0.32 V (recorded at 600 K). A similar behavior is observed for FF and efficiency which decreased from ~0.85 to ~16,234% (at 300 K) to 0.59 and 4.97% (at 600 K), respectively.

4. Conclusion

In this contribution, a newly proposed $ZnO/Si/Cu_2O$ heterostructure solar cell was studied by computer simulation using AMPS-1D software. We studied firstly the influence of thicknesses of different layers in the proposed structure and the acceptor concentration of p-Si absorber layer on the light J-V characteristics, in order to optimize the input parameters of the $ZnO/Si/Cu_2O$ solar cell. The impact of defects density of p-Si absorber layer and the operating temperature on the proposed $ZnO/Si/Cu_2O$ solar cell performance were also investigated. A 0.1 μm-ZnO/ 10 μm-Si/0.1 μm-Cu$_2$O heterostructure with N_A(p-Si) = 10^{19} cm^{-3}, showed a good characteristics: J_{SC} ~ 26.25 mA/cm^2, V_{OC} ~ 0.72 V, FF ~ 0.85 and η ~ 16.23%. These considered values were attributed to a low defect density of 1×10^{14}/cm^3 in p-Si absorber layer. By optimization, we realized a record efficiency for N_{def}(p-Si) lower than 10^{14}/ cm^3. For N_{def}(p-Si) = 10^{11}/cm^3 best characteristics have been estimated of about: J_{SC} ~ 27.57 mA/cm^2, V_{OC} ~ 0.78 V, FF ~ 0.90 and Eff ~ 21.78%. These results are very promising for defected $ZnO/Si/$ Cu_2O solar cells, and leave ample room in the future for further improvement.

Declaration of competing interest

The authors declare that they have no known competing financial interests or personal relationships that could have appeared to influence the work reported in this paper.
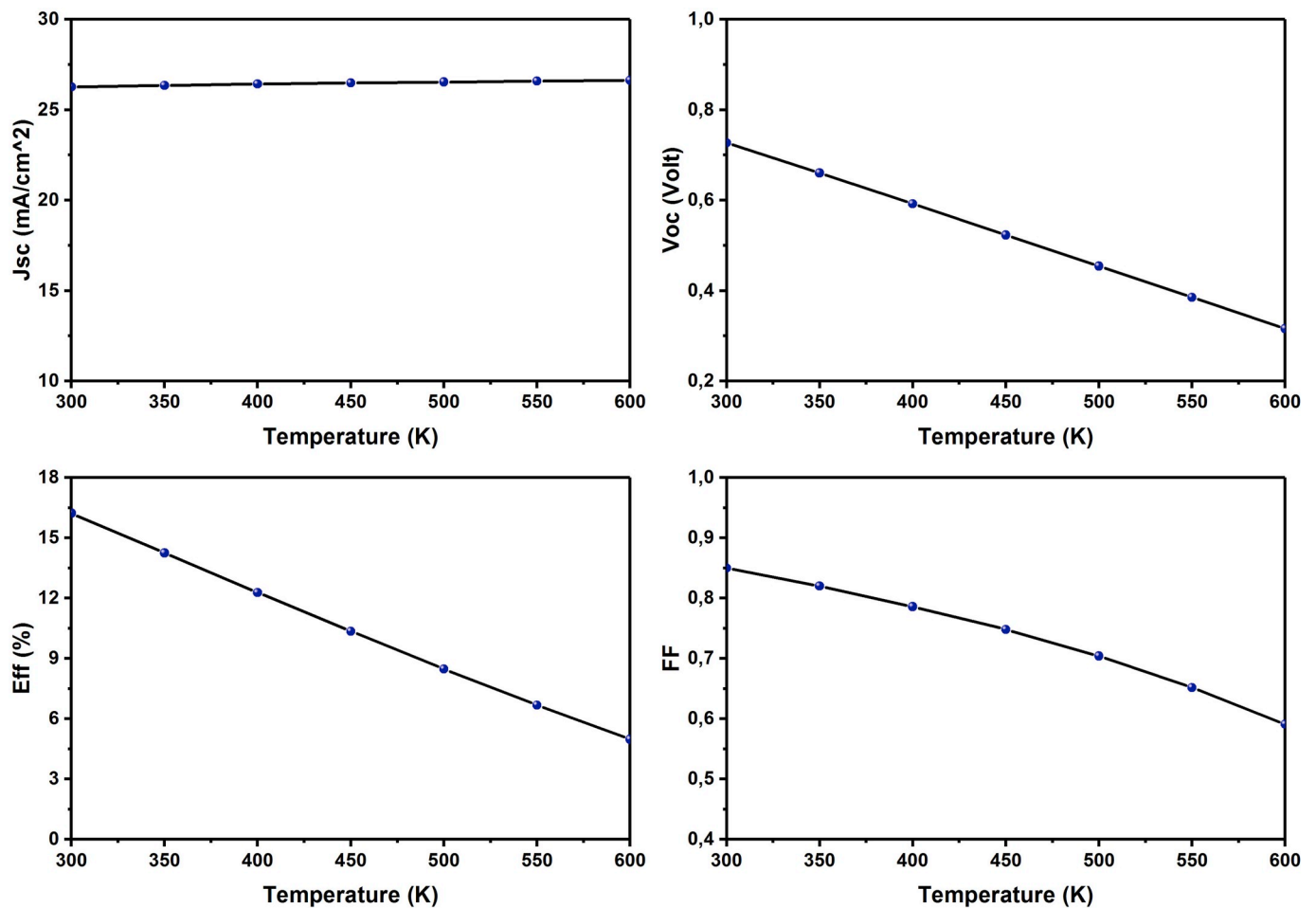
Fig. 10. Photovoltaic parameters of defected ZnO/Si/Cu$_2$O solar cell as a function of operating temperature.

Acknowledgements

References

[1] C.Q. Luo, F.C.C. Ling, M.A. Rahman, M. Phillips, C. Ton-That, C. Liao, K. Shih, J. Lin, H.W. Tam, A.B. Djurišić, S.-P. Wang, Surface polarity control in ZnO films deposited by pulsed laser deposition, Appl. Surf. Sci. 483 (2019) 1129–1135.

[2] A.B. Yadav, S. Jit, Particle size effects on the hydrogen sensing properties of Pd/ZnO Schottky contacts fabricated by sol–gel method, Int. J. Hydrogen Energy 42 (2017) 786–794.

[3] Y. Bicer, G. Chehade, I. Dincer, Experimental investigation of various copper oxide electrodeposition conditions on photoelectrochemical hydrogen production, Int. J. Hydrogen Energy 42 (2017) 6490–6501.

[4] H. Ennaceri, M. Boujnah, D. Erfurt, J. Rappich, X. Lifei, A. Khaldoun, A. Benyoussef, A. Ennaoui, A. Taleb, Influence of stress on the photocatalytic properties of sprayed ZnO thin films, Sol. Energy Mater. Sol. Cells 201 (2019), 110058.

[5] H.K. Juwhari, S.J. Ikhmayies, B. Lahlouh, Room temperature photoluminescence of spray-deposited ZnO thin films on glass substrates, Int. J. Hydrogen Energy 42 (2017) 17741–17747.

[6] M.R. Alfaro-Cruz, O. Ceballos-Sanchez, E. Luévano-Hipólito, L.M. Torres-Martínez, ZnO thin films deposited by RF magnetron sputtering: effects of the annealing and atmosphere conditions on the photocatalytic hydrogen production, Int. J. Hydrogen Energy 43 (2018) 10301–10310.

[7] A.M. Selman, M.A. Mahdi, Z. Hassan, Fabrication of Cu$_2$O nanocrystalline thin films photosensor prepared by RF sputtering technique, Phys. E Low-dimens. Syst. Nanostruct. 94 (2017) 132–138.

[8] F. Baig, Y.H. Khattak, B.M. Soucase, S. Beg, S. Ullah, Effect of anionic bath temperature on morphology and photo electrochemical properties of Cu$_2$O deposited by SILAR, Mater. Sci. Semicond. Process. 88 (2018) 35–39.

[9] E. Fortunato, V. Figueiredo, P. Barquinha, E. Elamurugu, R. Barros, Thin-film transistors based on p-type Cu$_2$O thin films produced at room temperature, Appl. Phys. Lett. 96 (2010), 192102.

[10] L. Liao, H.B. Lu, J.C. Li, C. Liu, D.J. Fu, Y.L. Liu, The sensitivity of gas sensor based on single ZnO nanowire modulated by helium ion radiation, Appl. Phys. Lett. 91 (2007), 173110.

[11] X. Wan, J. Wang, L. Zhu, J. Tang, Gas sensing properties of Cu$_2$O and its particle size and morphology-dependent gas-detection sensitivity, J. Mater. Chem. 2 (2014) 13641–13647.

[12] B. Cai, Y. Zhou, M. Zhao, H. Cai, Z. Ye, L. Wang, J. Huang, Synthesis of ZnO–CuO porous core–shell spheres and their application for non-enzymatic glucose sensor, Appl. Phys. A 118 (2015) 989–996.

[13] P.K. Pagare, A.P. Torane, Band gap varied cuprous oxide (Cu$_2$O) thin films as a tool for glucose sensing, Microchimica Acta 183 (2016) 2983–2989.

[14] E. Luévano-Hipólito, L.M. Torres-Martínez, D. Sanchez-Martinez, M.R. Alfaro-Cruz, Cu$_2$O precipitation-assisted with ultrasound and microwave radiation for photocatalytic hydrogen production, Int. J. Hydrogen Energy 42 (2017) 12997–13010.

[15] S. Bhatia, N. Verma, Photocatalytic activity of ZnO nanoparticles with optimization of defects, Mater. Res. Bull. 95 (2017) 468–476.

[16] H. Huang, J. Zhang, L. Jiang, Z. Zang, Preparation of cubic Cu$_2$O nanoparticles wrapped by reduced graphene oxide for the efficient removal of rhodamine B, J. Alloy. Comp. 718 (2017) 112–115.

[17] T. Zhou, Z. Zang, J. Wei, J. Zheng, J. Hao, F. Ling, X. Tang, L. Fang, M. Zhou, Efficient charge carrier separation and excellent visible light photoresponse in Cu$_2$O nanowires, Nano Energy 50 (2018) 118–125.

[18] P.-H. Hsiao, T.-C. Li, C.-Y. Chen, ZnO/Cu$_2$O/Si nanowire arrays as ternary heterostructure-based photocatalysts with enhanced photodegradation performances, Nanoscale Res Lett 14 (2019) 244.

[19] C.-H. Tang, K.-Y. Chen, C.-Y. Chen, Solution-processed ZnO/Si based heterostructures with enhanced photocatalytic performance, New J. Chem. 42 (2018) 13797–13802.

[20] C.-H. Tang, P.-H. Hsiao, C.-Y. Chen, Efficient photocatalysts made by uniform decoration of Cu$_2$O nanoparticles on Si nanowire arrays with low visible reflectivity, Nanoscale Res. Lett. 13 (2018) 312–319.

[21] M. Balık, V. Bulut, I.Y. Erdogan, Optical, structural and phase transition properties of Cu$_2$O, CuO and Cu$_2$O/CuO: their photoelectrochemical sensor applications, Int. J. Hydrogen Energy (2018), https://doi.org/10.1016/j.ijhydene.2018.08.159.

[22] Z. Zang, M. Wen, W. Chen, Y. Zeng, Z. Zu, X. Zeng, X. Tang, Strong yellow emission of ZnO hollow nanospheres fabricated using polystyrene spheres as templates, Mater. Des. 84 (2015) 418–421.

[23] Z. Zang, X. Tang, Enhanced fluorescence imaging performance of hydrophobic colloidal ZnO nanoparticles by a facile method, J. Alloy. Comp. 619 (2015) 98–101.

[24] J. Wei, Z. Zang, Y. Zhang, M. Wang, J. Du, X. Tang, Enhanced performance of light-controlled conductive switching in hybrid cuprous oxide/reduced graphene oxide (Cu$_2$O/rGO) nanocomposites, Opt. Lett. 42 (2017) 911–914.

[25] Z. Zang, Efficiency enhancement of ZnO/Cu$_2$O solar cells with well oriented and micrometer grain sized Cu2O films, Appl. Phys. Lett. 112 (2018), 042106.

[26] K.H. Han, M. Tao, Electrochemically deposited p-n homojunction cuprous oxide solar cells, Sol. Energy Mater. Sol. Cells 93 (2009) 153–157.

[27] Z. Zang, A. Nakamura, J. Temmyo, Single cuprous oxide films synthesized by radical oxidation at low temperature for PV application, Opt. Express 21 (2013) 11448–11456.

[28] A. Aissat, M.A. Ghomrani, W. Bellil, A. Benkouider, J.P. Vilcot, The doping effect on the properties of zinc oxide (ZnO) thin layers for photovoltaic applications, Int. J. Hydrogen Energy 40 (2015) 13685–13689.

[29] J. Xie, C. Guo, C.M. Li, Interface functionalization with polymer self-assembly to boost photovoltage of Cu$_2$O/ZnO nanowires solar cells, Int. J. Hydrogen Energy 39 (2014) 16227–16233.

[30] H. Heriche, Z. Rouabah, N. Bouarissa, New ultra thin CIGS structure solar cells using SCAPS simulation program, Int. J. Hydrogen Energy 42 (2017) 9524–9532.

[31] S. Boudour, I. Bouchama, N. Bouarissa, M. Hadjab, A study of CdTe solar cells using Ga-doped MgxZn1-xO buffer/TCO layers: simulation and performance analysis, J. Sci.: Adv. Mater. Devices 4 (2019) 111–115.

[32] S.B. Mitta, P. Murahari, K.R. Nandanapalli, D. Mudusu, R. Karuppannan, D. Whang, Si/ZnO heterostructures for efficient diode and water-splitting applications, Int. J. Hydrogen Energy 43 (2018) 16015–16023.

[33] S. Laidoudi, A.Y. Bioud, A. Azizi, G. Schmerber, J. Bartringer, S. Barre, A. Dinia, Growth and characterization of electrodeposited Cu$_2$O thin films, Semicond. Sci. Technol. 28 (2013), 115005.

[34] S.S. Jeong, A. Mittiga, E. Salza, A. Masci, S. Passerini, Electrodeposited ZnO/Cu$_2$O heterojunction solar cells, Electrochim. Acta 53 (2008) 2226–2231.

[35] T. Minami, Y. Nishi, T. Miyata, J. Nomoto, High-efficiency oxide solar cells with ZnO/Cu$_2$O heterojunction fabricated on thermally oxidized Cu$_2$O sheets, APEX 4 (2011), 062301.

[36] Y. Nishi, T. Miyata, T. Minami, The impact of heterojunction formation temperature on obtainable conversion efficiency in n-ZnO/p-Cu$_2$O solar cells, Thin Solid Films 528 (2013) 72–76.

[37] T.K.S. Wong, S. Zhuk, S. Masudy-Panah, G.K. Dalapati, Current status and future prospects of copper oxide heterojunction solar cells, Materials 9 (2016) 271.

[38] L. Zhu, G. Shao, J.K. Luo, Numerical study of metal oxide heterojunction solar cells, Semicond. Sci. Technol. 26 (2011), 085026.

[39] F.Z. Bedia, A. Bedia, B. Benyoucef, S. Hamzaoui, Electrical characterization of n-ZnO/p-Si heterojunction prepared by spray pyrolysis technique, Physics Procedia 55 (2014) 61–67.

[40] A.A. El-Amin, High efficiency computer simulation for Au/n-ZnO/p-Si/Al Schottky-type thin film heterojunctions, Siliconindia 9 (2017) 385–393.

[41] A. Aissat, M. El bey, R. Bestam, J.P. Vilcot, Modeling and simulation of Al$_x$Ga$_y$In$_{1-x-y}$As/InP quaternary structure for photovoltaic, Int. J. Hydrogen Energy 39 (2014) 15287–15291.

[42] S.J. Fonash, A manual for one-dimensional device simulation program (AMPS), Electron, in: Mater. Process. Res. Lab, Peensylvania State University, 2007.

[43] M. Reuter, W. Brendle, O. Tobail, J.H. Werner, 50 μm thin solar cells with 17.0% efficiency, Sol. Energy Mater. Sol. Cells 93 (2009) 704–706.

[44] J. Yoon, L. Li, A.V. Semichaevsky, J. Ha Ryu, H.T. Johnson, R.G. Nuzzo, J. A. Rogers, Flexible concentrator photovoltaics based on microscale silicon solar cells embedded in luminescent waveguides, Nat. Commun. 2 (2011) 343.

[45] J.L. Cruz-Campa, M. Okandan, P.J. Resnick, P. Clews, T. Pluym, R.K. Grubbs, V. P. Gupta, D. Zubia, G.N. Nielson, Microsystems enabled photovoltaics: 14.9% efficient 14 μm thick crystalline silicon solar cell, Sol. Energy Mater. Sol. Cells 95 (2011) 551–558.

[46] G. Li, Li He, J.Y.L. Ho, M. Wong, H.S.K. Kwok, Nanopyramid structure for ultrathin c-Si tandem solar cells, Nano Lett. 14 (2014) 2563–2568.

[47] M. Pavan, S. Rühle, A. Ginsburg, D.A. Keller, H.N. Barad, P.M. Sberna, D. Nunes, R. Martins, A.Y. Anderson, A. Zaban, E. Fortunato, TiO2/Cu2O all-oxide heterojunction solar cells produced by spray pyrolysis, Sol. Energy Mater. Sol. Cells 132 (2015) 549–556.

[48] M.H. Tran, J.Y. Cho, S. Sinha, M.G. Gang, J. Heo, Cu2O/ZnO heterojunction thin-film solar cells: the effect of electrodeposition condition and thickness of Cu2O, Thin Solid Films 661 (2018) 132–136.

[49] O. Isabella, K. Jäger, A. Smets, R. van Swaaij, M. Zeman, Solar Energy: the Physics and Engineering of Photovoltaic Conversion, Technologies and Systems, UIT Cambridge, 2016.

[50] D. Yan, A. Cuevas, Empirical determination of the energy band gap narrowing in highly doped n+ silicon, J. Appl. Phys. 114 (2013), 044508.

[51] F.E. Rougieux, C. Sun, D. Macdonald, Determining the charge states and capture mechanisms of defects in silicon through accurate recombination analyses: a review, Sol. Energy Mater. Sol. Cells 187 (2018) 263–272.